

Synthesis, Characterization, and Application of Cationic Water-Soluble Oligofluorenes in DNA-Hybridization Detection

Bin Liu* and Shudipto Konika Dishari^[a]

Abstract: A simple and efficient approach was developed for the synthesis of a series of cationic water-soluble oligofluorenes up to a chain length of a heptamer. Bromoalkyl-substituted fluorenyl boronic esters as the key intermediates were synthesized by using a modified Miyaura reaction. With an increasing number of repeat units (trimer to hexamer), the size-specific oligomers have shown redshifts in both the absorption and emission maxima. The emission maximum reaches the limit

for the hexamer in both water and buffer solution. The quantum yields of the oligomers decreased with increased oligomer size in water. Both fluorescence quenching of the oligomers by 9,10-anthraquinone-2,6-disulfonate and the fluorescence resonance energy

Keywords: DNA • fluorescein • fluorescence quenching • fluorescence resonance energy transfer (FRET) • oligofluorenes

transfer experiments with the oligomers as the donor and fluorescein (Fl)-labeled double-stranded DNA (dsDNA-Fl) as the acceptor revealed the chain-length-dependent behavior. The Stern–Volmer quenching constant increased with the molecular size, whereas the highest donor-sensitized Fl emission was observed for the hexamer. These size-specific oligomers also served as a model to study the structure–property relationships for cationic polyfluorenes.

Introduction

Water-soluble conjugated polymers (CPs) as optically sensitive materials have been widely used in chemical and biological sensors.^[1] Cationic conjugated polymers (CCPs), in particular, have been proven useful for strand-specific DNA detection by taking advantage of the light-harvesting properties of conjugated polymers and the fluorescence resonance energy transfer (FRET) between the polymers and dye molecules attached to PNA, DNA, or peptide.^[2] The same strategy has also been used to detect RNA, protein, and other small molecules in aqueous media and on a solid substrate.^[3]

Efficient fluorescence resonance energy transfer from the cationic conjugated polymer to the dye is a required condition for high sensitivity.^[4] Maximized spectral overlap between the donor emission and the acceptor absorption, improved orientation, and a shortened distance between the donor and the acceptor should lead to more-efficient

FRET.^[5] Our previous studies have shown that both CCP backbone structure and the side chain length affect energy-transfer efficiencies.^[6] Improved signal amplification has been demonstrated with shape-adaptable polymers in which more conformational freedom and improved registry with the analyte shape favor more-efficient FRET.^[6a] The importance of matching energy levels between the donor–acceptor pairs to minimize photo-induced charge-transfer processes that compete with the desired FRET amplification was also reported.^[7] Recently, we also developed a nanoparticle-based sensing strategy in which the energy-waste channel of dye self-quenching upon CCP/DNA–dye complexation was minimized. The collective response from polymers self-assembled on the nanoparticle surface provided a signal amplification of the dye emission by over 110-fold.^[8] Efforts have also been made to tune the conjugated polymer emission to match different probe chromophores^[6b] and to change the solvent media for maximized signal amplification.^[9]

Despite much success in demonstrating the sensing strategy and improving the CCP-based sensor performance, fundamental information concerning important relationships between structure and optical properties in cationic water-soluble conjugated polymer solutions remain lacking.^[10,6c] Structural uncertainties in these polymers, such as the molecular-weight distribution, batch-to-batch variation in mo-

[a] Prof. B. Liu, S. K. Dishari
Department of Chemical and Biomolecular Engineering
National University of Singapore
Singapore 117576 (Singapore)
E-mail: cheliub@nus.edu.sg

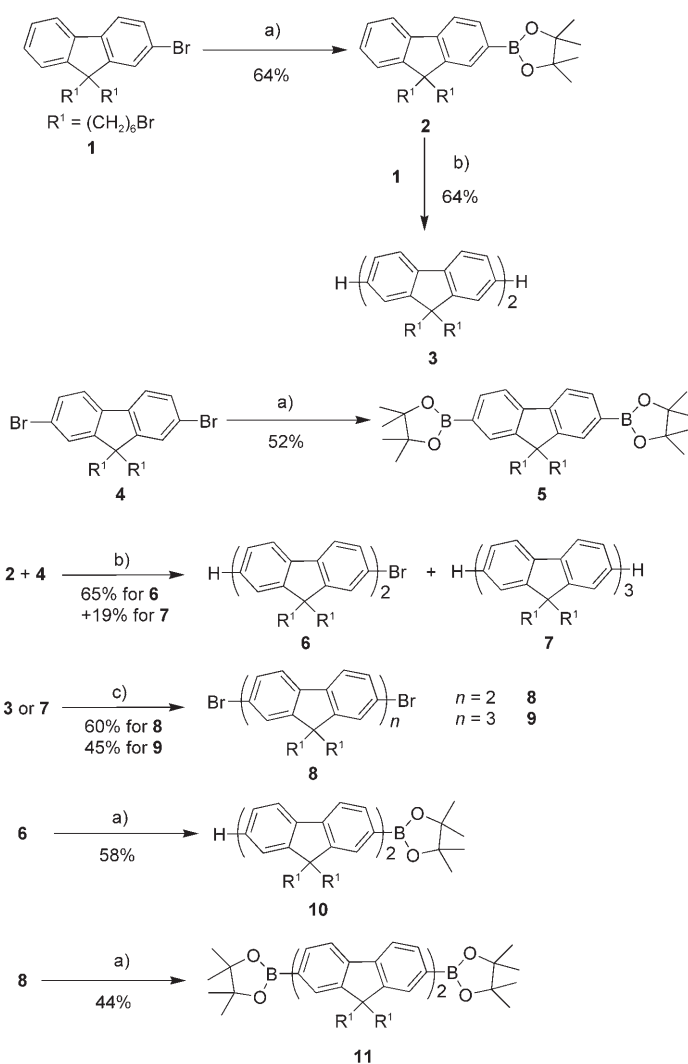
Supporting information for this article is available on the WWW under <http://dx.doi.org/10.1002/chem.200800216>.

molecular weight, and defects prevent detailed study of the structure–property relationships of CCPs and the chain-length-dependent energy transfer/electron transfer between donor molecules and dye-labeled biomolecules involved in the FRET process. In the previous effort, water-soluble fluorene-phenylene oligomers with one, two, or three fluorene units on both sides of the phenylene ring were synthesized to study the interactions between the oligomers and single-stranded DNA (ssDNA) or double-stranded DNA (dsDNA).^[10b] Although the oligomer size was found to affect the energy-transfer ratios of oligomer/ssDNA-fluorescein (Fl) to oligomer/dsDNA-Fl, the relationship between the molecular size and the oligomer-sensitized Fl emission intensity for dsDNA-Fl or ssDNA-Fl was not clear. In addition, the changes in the optical properties of the oligomers and their response to DNA molecules could not be generalized to understand the polymer behavior as the oligomers do not have the same repeat unit. Better understanding of cationic conjugated polymers and the chain-length-dependent electron- and energy-transfer processes is thus of high importance to provide guidance for further improvement in CCP-based sensor performance.

Herein, we describe the synthesis and characterization of a series of cationic water-soluble conjugated oligofluorenes with a chain length that varies from three units (trimer) to seven units (heptamer). These molecules were used to examine the chain-length-dependent optical properties of water-soluble polyfluorenes and served to illustrate how variations in conjugation length could be used to optimize the fluorescence-based sensory process. We started with the synthesis and examination of the optical properties of the oligomers. This was followed by the study of oligomer-quenching behaviors in the presence of 9,10-antraquinone-2,6-disulfonate and the energy-transfer processes from the oligomers to dsDNA-Fl. Poly[9, 9-bis(6'-(*N,N,N*-trimethylammonium)-hexyl)fluorene] dibromide] was also studied to allow a comparison of the oligomers against the polymer structure.

Results and Discussion

The intermediates for water-soluble oligomers were obtained by the sequence of reactions shown in Scheme 1. Starting from the mono- (**1**) and dibromide (**4**) of bromohexyl-substituted fluorene, the corresponding mono- **2** and diboronic esters **5** were synthesized by the modified Miyaura reaction in the presence of bis(pinacolato)diboron and KOAc by using dioxane as the solvent. Compounds **2** and **5** were obtained in a yield of 64 and 52%, respectively, after purification by silica chromatography. Suzuki coupling between one equivalent of **1** and **2** with [Pd(PPh₃)₄] as the catalyst in a mixture of toluene/2M K₂CO₃ aqueous solution for 24 h yielded the fluorenyl dimer **3** in 64% yield. Similarly, reaction of **2** with 1.5 equivalents of **4** gave the monobrominated fluorenyl dimer **6** in 65% yield, together with a small fraction of trimer **7** in 19% yield. Compound **7** was also synthesized from two equivalents of **2** and one equivalent of **4**

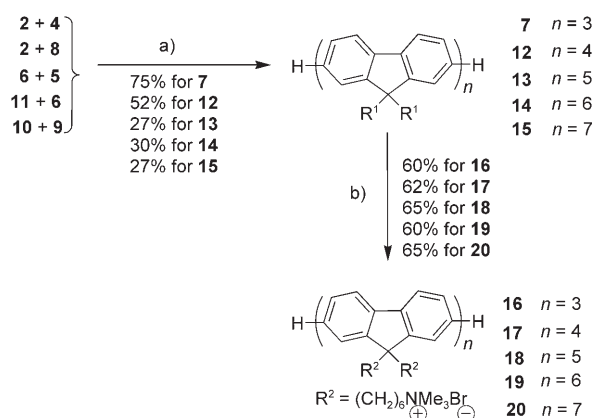


Scheme 1. Synthetic route to the intermediates for the oligomers. a) bis(pinacolato)diboron, [PdCl₂(dppf)], KOAc, dioxane, 80 °C; b) [Pd(PPh₃)₄], 2M K₂CO₃, toluene/H₂O, 100 °C; c) Br₂/I₂, dichloromethane. dppf = 1,1'-bis(diphenylphosphino)ferrocene.

in 75% yield. Direct bromination of **3** and **7** at room temperature by using liquid bromine in dichloromethane in the presence of a trace amount of iodine afforded dibrominated fluorenyl dimer **8** and trimer **9** in a yield of 60 and 45%, respectively, after purification. For large bromide molecules, such as **9**, multiple column chromatography was necessary for purification as the side products were difficult to remove through recrystallization. Compounds **6** and **8** were transformed to their corresponding boronic esters **10** and **11** in a yield of 58 and 44%, respectively, by using the same method as for **2** and **5**. The availability of the alkyl bromide containing arylboronates simplified the synthesis of precursors for water-soluble conjugated molecules that rely on Suzuki cross-coupling protocols. Furthermore, the new procedure bypassed the need to prepare trialkylamino-substituted oligomers or protected intermediates, which were complicated or difficult to purify.^[10] As compared with pre-

vious approaches for neutral monodispersed oligofluorenes,^[11] which took advantage of the large reactivity difference between diazonium salts or trimethylsilyl groups and aryl bromides in the cross-coupling reaction with aryl boronates,^[12] our strategy is much more straightforward and is compatible with functional bromide groups at the end of the side chain.

As shown in Scheme 2, the synthetic entry to the fluorenyl oligomers that range from the trimer to the heptamer involved a palladium-mediated Suzuki cross-coupling reaction



Scheme 2. Synthetic route to the neutral and water-soluble oligomers. a) $[\text{Pd}(\text{PPh}_3)_4]$, 2 M K_2CO_3 , toluene/ H_2O , 100 °C; b) NMe_3 , THF/ H_2O .

between the fluorenyl boronic esters and the brominated fluorenes. The reactions proceeded in the presence of $[\text{Pd}(\text{PPh}_3)_4]$ in a mixture of 2 M aqueous K_2CO_3 solution and THF or toluene. The coupling between two equivalents of **2** and **4** or **8** afforded fluorenyl trimer **7** and tetramer **12** in a yield of 75 and 52%, respectively. The fluorenyl pentamer **13** and hexamer **14** were obtained from a coupling reaction between **5** or **11** and two equivalents of **6**, both in a yield of approximately 30%. Similarly, the heptamer **15** was obtained in 27% yield by coupling **9** and **10**. For fluorenyl oligomers, purification was done by using column chromatography followed by recrystallization from hexane–dichloromethane to afford the products as white or pale yellow solids. Results from ^1H and ^{13}C NMR spectroscopy, MALDI-TOF mass spectrometry, and elemental analysis confirmed the right molecular structures and high purity of the neutral oligomers of **7** and **12–15**. Quaternization of the pendant bromide groups on the backbone, by addition of condensed trimethylamine, provided the cationic water-soluble oligomers **16–20** in a yield of 60–65% after precipitation from acetone and subsequent drying. After quaternization, the characteristic signals at $\delta = 3.40\text{--}3.20$ ppm, which correspond to the chemical shift of $-\text{CH}_2\text{CH}_2\text{Br}$ for the neutral oligomers, disappeared completely. A new signal at $\delta \approx 3.60$ ppm, which is assigned to $-\text{CH}_2\text{CH}_2\text{N}(\text{CH}_3)_3$, appeared in the ^1H NMR spectra of **16–20**. The degree of quaternization is thus nearly quantitative for the oligomers. The molecular structures of **16–20** were also confirmed by using NMR

spectroscopy and MALDI-TOF mass spectrometry. By using the hexamer as an example, observed ionized mass peaks correspond to 441.79 $[\text{M}-7\text{Br}]^{7+}$, 377.36 $[\text{M}-8\text{Br}]^{8+}$, 254.06 $[\text{M}-11\text{Br}]^{11+}$, and 224.54 $[\text{M}-12\text{Br}]^{12+}$. The polymer has a number-average molecular weight of 33000 (ca. 50 repeat units) and a polydispersity of 1.8. Oligomers **16–18** are highly soluble in water ($>20\text{ mg mL}^{-1}$), whereas oligomers **19** and **20** require ultrasonication to get a clear aqueous solution with a concentration of 20 mg mL^{-1} . The polymer has a low solubility in water ($<2\text{ mg mL}^{-1}$).

The absorption spectra of the oligomers **16–20** and the polymer in water with the same fluorene unit concentration of $3.0 \times 10^{-6}\text{ M}$ are shown in Figure 1 and the data are presented

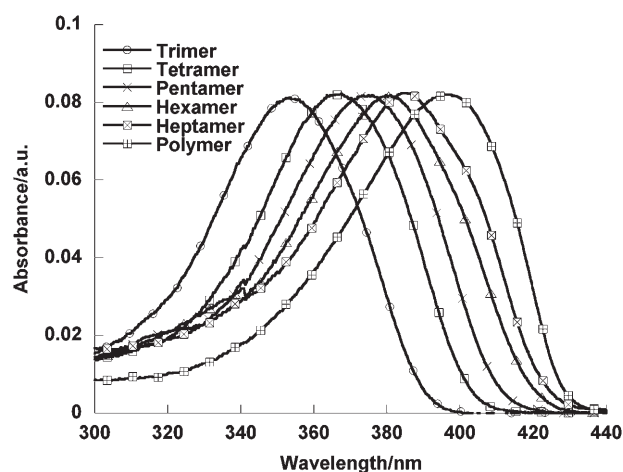


Figure 1. The absorption spectra of the fluorenyl oligomers **16–20** and the polymer in water with $[\text{fluorene unit}] = 3.0 \times 10^{-6}\text{ M}$.

in Table 1. The corresponding absorption spectra in methanol are shown in Figure S1 in the Supporting Information. The fluorenyl oligomers exhibit an unstructured absorption band in both water and methanol. There is a progressive redshift in the absorption maxima with increasing chain length in both water and methanol. In water, the maximum absorption wavelength increases from 353 nm for the trimer to 385 nm for the heptamer and 395 nm for the polymer, which is slightly redshifted as compared with that in methanol. Previous studies have shown that methanol is a good solvent for amphiphilic oligomers and polymers, which can greatly reduce molecular aggregation in water.^[13] In methanol, the absorption maxima for the trimer to the heptamer are 350, 364, 371, 375, and 379 nm, respectively, which correspond to the energies of 3.54, 3.41, 3.34, 3.31, and 3.27 eV. From the absorption maximum for each oligomer in methanol, it is possible to determine the active conjugation length of the polymer by examination of the plot of the absorption energy versus the value of $1/n$, where n represents the number of fluorene units for each oligomer. As shown in Figure 2, the absorption energy versus n gives a linear curve (correlation coefficient = 0.996) from which one can derive Equation (1):

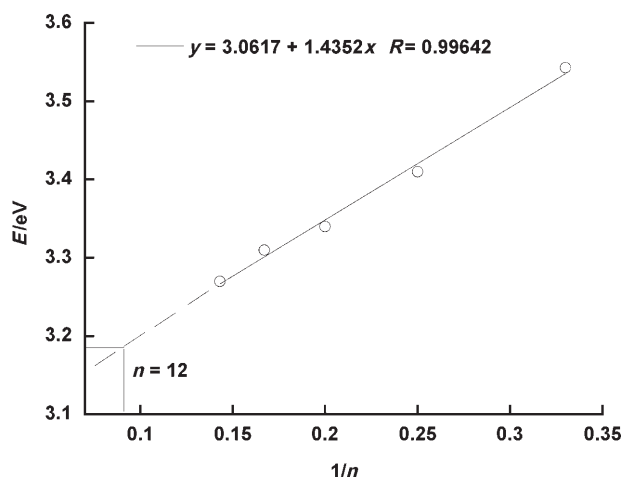


Figure 2. Energy of the oligomer absorption maxima in methanol versus the inverse ring number of fluorenyl oligomers.

$$E(\text{eV}) = 3.06 + 1.435/n \quad (1)$$

From the absorption maximum of the polymer (390 nm, which corresponds to 3.18 eV), one can estimate that the cationic polyfluorene has an effective conjugation length of about 11 to 12 repeat units. This is similar to the previous report in which an effective conjugation length of 12 repeat units was reported for poly(9,9-di-*n*-hexylfluorene-2,7-diyl), which showed an absorption maximum of 390 nm in tetrahydrofuran.^[14] The molar absorption coefficient (ϵ) based on the fluorene unit is nearly the same for all the oligomers and the polymer in water, which has a value of approximately $2.9 \times 10^4 \text{ L mol}^{-1} \text{ cm}^{-1}$. In methanol, the ϵ based on the fluorene unit is approximately $3.0 \times 10^4 \text{ L mol}^{-1} \text{ cm}^{-1}$, which is slightly higher than that in water.

The emission spectra of the oligomers and the polymer were also studied in both water (Figure 3) and methanol (Figure S1 in the Supporting Information), and the data are summarized in Table 1. In water, the emission maxima of

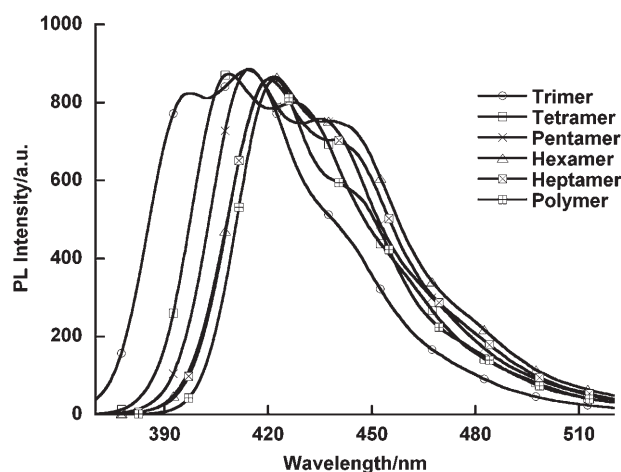


Figure 3. The emission spectra of the fluorenyl oligomers **16–20** and the polymer in water at $[\text{fluorene unit}] = 3.0 \times 10^{-6} \text{ M}$.

the oligomers increase from 396 nm for the trimer to 422 nm for the hexamer, and the emission maxima remain virtually unchanged when the chain length is further increased. The fact that the spectral absorption maxima continue to redshift up to $n = 12$, whereas the emission maximum does not shift further to the red for $n > 6$, suggests that the fluorene backbone geometry changes significantly in going from the ground state (S_0) to the vibronically relaxed excited state.^[14] Similar observation has also been reported previously in which the emission maximum of neutral oligofluorenes in tetrahydrofuran reaches the limit at $n = 6$.^[14] In methanol, the emission maxima are slightly blueshifted for all the oligomers and the polymer, and the emission spectra are narrower as compared with those in water. The narrowed emission spectra reflect a smaller conformational distribution of excited species for **16–20** in methanol, as compared with that in water. Both the oligomers and the polymer have shown well-structured PL spectra in water and in methanol. As shown in Figure 3, for each molecule, two well-resolved emission bands that correspond to 0–0 and 0–1 intrachain singlet transition are present. The ratio of the intensities for the 0–0 transition to the 0–1 transition increases with oligomer size. When normalized, the polymer shows the lowest 0–1 transition. This is due to the increased intrachain coupling with increased chain length.^[12a] The fluorescence quantum efficiency (Φ) was determined against quinine sulfate in 0.1 M H_2SO_4 (54%) as the standard, and the values are shown in Table 1. The Φ values of the oligomers decrease with increasing chain length in both water and methanol. The Φ value varies from 94% for the trimer to 78% for the polymer in methanol, and from 90% for the trimer to 45% for the polymer in water, respectively.

Understanding the optical properties of the oligomers and the polymer in water with varying ionic strength is of high importance for bioassay applications as buffer ions screen negative charges on DNA, which facilitate hybridization.^[15] The effect of ionic strength on the optical properties of the oligomers and the polymer was studied by monitoring the absorption and emission spectral changes of their aqueous solutions upon addition of different amounts of NaCl. In these experiments, the solution concentration based on the fluorene unit was kept at $3 \times 10^{-6} \text{ M}$, with $[\text{NaCl}]$ varying from 0 to 118 mM at an increase of 12 mM upon each NaCl addition. The corresponding spectra are shown in Figure S2 and S3 in the Supporting Information. With the addition of NaCl, there was a decrease in both absorption and fluorescence for all solutions. When the concentration of NaCl was varied from 0 to 118 mM, the decrease in absorbance was similar (around 40%) for all solutions and there was no obvious precipitation observed. For the trimer and tetramer, a slight redshift was also observed with increased NaCl concentration in solution. For the pentamer, hexamer, heptamer, and the polymer, the absorption spectra also changed their shapes even in the presence of 12 mM NaCl. A new shoulder peak appeared at long wavelength and the peak intensity increased with increased chain length. The most obvious change was observed for the polymer in which the ab-

sorption at 395 nm in water slightly redshifted to 397 nm in the presence of NaCl and a more-intense new band appeared at 411 nm. The changes in the absorption spectra of **16–20** and the polymer upon addition of NaCl reveals that the conformational changes in the ground state is more obvious for large-size molecules.

In general, when molecules aggregate and if the aggregates are soluble, bathochromic and hypsochromic shifts are observed for the absorption when the unaggregated form is compared with the aggregated forms.^[16] On the other hand, when molecules aggregate and the aggregates are not very soluble, aggregation or precipitation can result in a decrease in the absorption band and an increase in the absorption at the long wavelength side owing to particle scattering. Neither of these two effects are obvious in Figure S2 in the Supporting Information, which indicates that the observed spectral change is less likely to be due to salt-induced aggregation. The effect of NaCl on the effective diameters (EDs) of the oligomers and the polymer in solution was also studied by dynamic light-scattering techniques.^[17] At an equal [fluorene unit] = 1×10^{-5} M in water, the EDs for solutions containing the trimer to the heptamer were in the range of 350–450 nm, and the ED for the polymer was around 600 nm. These values did not change within 24 h. Upon addition of 118 mM NaCl to each solution, the change in ED was less than 5% when measured within 5 min. However, the EDs increased to approximately 1000 nm or more for all solutions when they were kept at room temperature for 24 h. This indicates that the spectral redshift and the decrease in absorbance in the presence of NaCl (shown in Figure S2 in the Supporting Information) are not attributed to aggregation formation. The new band (>400 nm) in the presence of NaCl reflects the changes of the backbone conformation of the oligomers/polymer from a more disordered state to a less disordered state in solution.^[18] The conformational change could favor molecular agglomeration and aggregation, which eventually leads to big aggregates and precipitation when the solutions are kept for a long time.

Upon addition of NaCl to the oligomer/polymer solutions, a redshift in emission was also observed for aqueous solutions containing the pentamer, hexamer, heptamer, and the polymer. The redshift also continued with increased NaCl concentration. The rate of the decrease in fluorescence also increased with the molecular size. When the NaCl concentration was increased from 0 to 118 mM, a 40% decrease in fluorescence intensity was observed for the trimer, whereas a 90% decrease was observed for the polymer. The quantum yield of the trimer did not change significantly with the increased ionic strength in solution. The most obvious decrease in quantum yield was observed for the polymer,

which changed from 45% in water in the absence of NaCl to about 8% at [NaCl] = 118 mM in solution. Quantitative analysis of the changes in fluorescence quantum yield requires lifetime measurement and calculation of radiative and non-radiative decay rates, which is currently under study. In the following studies, 25 mM phosphate buffer solution (pH 7.4) was used as the medium, which was chosen to maintain not only a relatively high fluorescence quantum yield for all the donor molecules but also good stability of double-stranded (ds)DNA in solution.^[7,19] The absorption and emission spectra of the oligomers and the polymer in buffer solution are shown in Figure S4 in the Supporting Information, and the corresponding data are summarized in Table 1.

Table 1. Summary of the absorption and emission spectra for the fluorenyl oligomers and the polymer in methanol, water, and buffer solution (25 mM phosphate buffer solution; pH 7.4).

Compounds	Methanol			Water			Buffer solution		
	$\lambda_{\max(\text{abs})}$	$\lambda_{\max(\text{em})}$	Φ [%]	$\lambda_{\max(\text{abs})}$	$\lambda_{\max(\text{em})}$	Φ [%]	$\lambda_{\max(\text{abs})}$	$\lambda_{\max(\text{em})}$	Φ [%]
trimer	350	392	94	353	396	90	354	398	82
tetramer	364	404	90	367	408	89	372	412	72
pentamer	371	410	88	374	415	82	379	423	67
hexamer	375	412	85	380	422	70	383	426	57
heptamer	380	413	80	385	422	52	386	426	46
polymer	390	414	78	395	422	45	411	428	17

To investigate the electronic communication and chain-length dependent light-harvesting properties, it is useful to examine the processes such as the fluorescence quenching and energy transfer with different acceptor molecules. Fluorescence quenching of the oligomers and the polymer was examined by using the electron acceptor 9,10-anthraquinone-2,6-disulfonate (AQS²⁻) in 25 mM phosphate buffer solution. Experiments were conducted at an equal concentration of the fluorene unit of 2×10^{-6} M. The quenching efficiency is determined by using the Stern–Volmer equation: $F_0/F = 1 + K_{sv}[\text{quencher}]$, where F_0 and F are fluorescence intensities in the absence and presence of the quencher, respectively. The K_{sv} plot of the oligomers quenched by AQS²⁻ in buffer solution is shown in Figure 4. The Stern–Volmer constants (K_{sv}) obtained from the linear region of the Stern–Volmer plot of F_0/F versus [AQS²⁻] are 2.07×10^7 , 2.35×10^7 , 3.25×10^7 , 3.57×10^7 , 3.89×10^7 , and 6.20×10^7 , for the trimer to the heptamer and the polymer, respectively. Such a high K_{sv} value is due to the static quenching by formation of the ground-state complexes through charge pairing.^[20] Different from previous studies in which only K_{sv} between a small oligomer and a polymer was compared, our study indeed provided more-detailed evidence to indicate that there was a gradual increase in K_{sv} with the increased chain length of donor molecules.^[10a,21] This result suggests that the ability of an oligomer/polymer to harvest light and deliver excitons to the acceptors improves as the backbone chain length increases. Higher K_{sv} values for larger-size molecules reflect more-efficient intra- and inter-chain electron-transfer mechanisms with the increased chain length. This

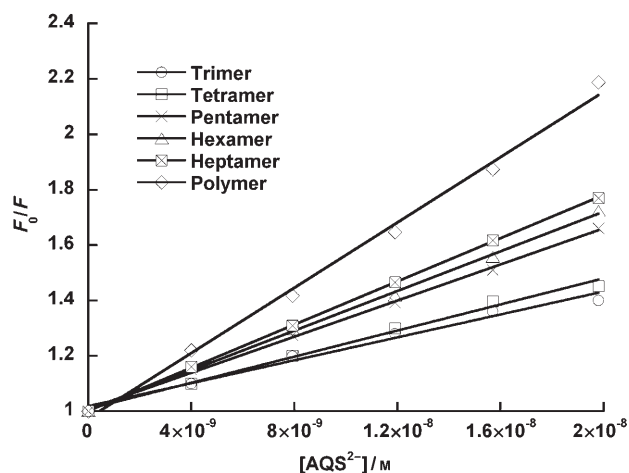


Figure 4. K_{sv} plots of the oligomers and the polymer quenched by AQS^{2-} in 25 mM phosphate buffer solution. [fluorene unit] = 2×10^{-6} M.

phenomena could be explained in terms of the “molecular wire effect” in which a single quencher can effectively quench many repeat units for the large-size molecules.^[22]

FRET experiments between the oligomers/polymer (donor) and a low-energy acceptor were also performed. FI was chosen as the acceptor because there was a spectral overlap between the absorption of FI and the emission of the oligomers/polymer. FI was attached to a dsDNA to ensure the electrostatic interaction that could bring the donor molecules and FI into close proximity for energy transfer. The dsDNA was obtained through hybridization of a FI-labeled single-stranded (ss)DNA (5'-FI-ATC TTG ACT ATG TGG GTG CT-3') with its complementary strand (5'-AGC ACC CAC ATA GTC AAG AT-3'). A comparison of the FI emission intensity by excitation of the donors at their absorption maxima is shown in Figure 5. The donor emission tail in the FI emission region (500–700 nm) was subtracted from the donor-sensitized FI emission. As shown

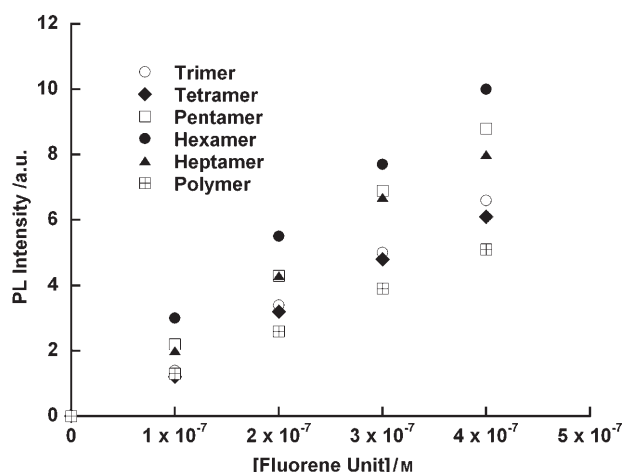


Figure 5. Fluorescence intensity of the donor-sensitized dsDNA-FI emission with varying oligomer/polymer concentrations based on fluorene units. [dsDNA] = 2×10^{-8} M.

in Figure 5, there was an increase in FI emission upon addition of all the donors to dsDNA-FI ([dsDNA-FI] = 1×10^{-8} M) when [fluorene unit] was in the range of $0-4 \times 10^{-7}$ M. This observed increase in FI emission was due to the increased number of fluorene units that were associated with dsDNA-FI, and were within a valid FRET distance. The FI emission intensity almost saturated at [fluorene unit] = 4×10^{-7} M, which corresponded to a charge ratio (positive charges of donors to the negative charges of dsDNA) close to 1. Within the tested donor concentration range, the most intense donor-sensitized FI emission was observed for the hexamer, and the lowest was observed for the polymer. The data in Figure 5 demonstrate that the intensity of donor-sensitized FI signals follows the following trend: hexamer > pentamer > heptamer > tetramer ≈ trimer > polymer. By using the spectral data (shown in Figure S4 in the Supporting Information) and the donor quantum yields in the buffer solution (shown in Table 1), the Förster distance (R_0)^[23] was calculated to be 42.8, 43.8, 44.5, 44.8, 43.9, and 37.4 Å for the trimer to heptamer and the polymer, respectively, assuming an orientation factor (κ^2) of 2/3. The R_0 for the polymer/fluorescein is similar to that of 37.2 Å, which was reported for a polyfluorene derivative/fluorescein pair.^[24] According to Figure S4 in the Supporting Information, the overlap between the emission of the trimer and the absorption of fluorescein is obviously smaller than that for the others, the high quantum yield of the trimer in buffer solution compensates for the small spectral overlap, which leads to an R_0 value that is only slightly smaller than other oligomers. Interestingly, the hexamer-sensitized FI emission was almost two times higher than that from the trimer, despite a lower quantum yield for the hexamer. As the number of fluorene units was kept constant in all the experiments, the difference in donor-sensitized FI emission should be mainly attributed to the improved spectral overlap between large oligomers and FI. Further increases in the molecular size from the hexamer to the polymer do not contribute to the spectral overlap as the emission maximum reaches the limit for the hexamer in the buffer solution. In addition to the higher donor-sensitized FI emission, the hexamer also provides a higher selectivity for dsDNA-FI/ssDNA-FI as compared with that for the polymer. The results are shown in Figure S5 in the Supporting Information.

Conclusion

In summary, we have presented an efficient approach to synthesize water-soluble oligofluorenes up to the heptamer length. Both the absorption and emission maxima of the oligomers redshifted with increased chain length, and the emission maximum reached the limit for the hexamer. The fluorescence quantum yields of the oligomers decreased with increased molecular size and were higher in water than in buffer solution. Fluorescence-quenching experiments demonstrated higher quenching rates with increased chain length, whereas the FRET experiments showed that the

hexamer was the best donor for sensitized fluorescein emission. Comparison of the optical properties and sensing behaviors between the oligomers and the polymer revealed the importance of molecular size in biosensing applications. As compared with the oligomers, fluorescence quenching of the polymer was more efficient, which is due to the “molecular-wire effect” in which a single quencher could effectively quench many repeat units for large molecules. For bioapplications that take advantage of fluorescence quenching of conjugated molecules, polymers could be more efficient platforms than oligomers. On the other hand, less-efficient signal amplification was demonstrated for the polymer, which was due to the low quantum yield of the polymer in buffer solution. Comparison between the polymer and the hexamer also showed higher selectivity between ssDNA and dsDNA for the hexamer. Designing new optical platforms will require balancing of the properties of size, spectral overlap, and the quantum yield. Small molecules tend to have higher quantum yields and are less sensitive to solvent media (i.e. ionic strength), but they generally show less spectral overlap than their larger counterparts. Large-size oligomers have the advantage of high purity, high quantum yields, little aggregation, and have shown similar spectral overlap to acceptors as compared with polymers. The oligomer approach could serve as a new strategy to provide more-efficient donors for conjugated polymer-based bioassay applications.

Experimental Section

General methods: Chemicals were purchased from Aldrich and used without further purification. ^1H NMR and ^{13}C NMR were recorded on Bruker 400 Ultrashield.TM. Shimadzu UV-1700, UV-Vis spectrophotometer was used to measure the absorption spectra. PL spectra were measured on Perkin Elmer LS55 luminescence spectrometer. The mass spectra were obtained by using a Bruker Daltonics Autoflex II TOF system. MALDI-TOF was performed by using 2, 5-dihydroxybenzoic acid (DHB) as the matrix under the reflector mode for data acquisition. THF and 50% CH_3OH (50% H_2O) were used as solvents for neutral and charged compounds, respectively. 2-Bromo-9,9-bis(6'-bromohexyl)fluorene (**1**) and 2,7-dibromo-9,9-bis(6'-bromohexyl)fluorene (**4**) were synthesized according to the previous report.^[6c,13a]

2-[9,9-Bis(6-bromohexyl)fluorenyl]-4,4,5,5-tetramethyl[1.3.2]dioxaborolane (2): 2-Bromo-9,9-bis(6'-bromohexyl)fluorene (**1**; 4.54 g, 7.95 mmol), bis(pinacolatodiboron) (3.02 g, 11.93 mmol), and potassium acetate (2.94 g, 29.82 mmol) were placed in a 100-mL round bottom flask. Anhydrous dioxane (80 mL) and $[\text{PdCl}_2(\text{dppf})]$ (0.20 g, 0.24 mmol) were added to the flask and the reaction vessel was degassed. The mixture was stirred at 80°C for 12 h under nitrogen. After the mixture had been cooled to room temperature, dioxane was removed by rotary evaporation. The residue was extracted with dichloromethane, and the organic phase was washed with water and brine, and dried over magnesium sulfate. The solvent was removed and the residue was purified by silica gel column chromatography (dichloromethane/hexane=1:2) to afford **2** (3.13 g, 64%) as white crystals. ^1H NMR (400 MHz, CDCl_3): δ =7.83–7.70 (m, 4H), 7.35–7.32 (m, 3H), 3.28–3.25 (t, J =7.2 Hz, 4H), 2.03–1.95 (m, 4H), 1.67–1.58 (q, 4H), 1.40 (s, 12H), 1.18–1.16 (q, 4H), 1.05–1.03 (m, 4H), 0.63–0.55 ppm (m, 4H); ^{13}C NMR (100 MHz, CDCl_3): δ =151.1, 149.7, 144.3, 141.1, 134.0, 128.9, 127.8, 127.0, 123.0, 120.4, 119.3, 83.9, 55.1, 40.3, 34.2, 32.8, 29.2, 27.9, 25.2, 23.6 ppm; MS (EI): m/z (%): 618.90 [M^+].

9,9,9',9'-Tetrakis(6'-bromohexyl)-2,2'-bifluorene (3): A flask charged with compound **1** (0.61 g, 0.99 mmol), compound **2** (0.58 g, 0.99 mmol), and potassium carbonate (0.68 g, 4.93 mmol) in toluene (8 mL) and water (3 mL) was degassed for 15 min. $[\text{Pd}(\text{PPh}_3)_4]$ (0.02 g) was added to the flask and the mixture was degassed for another 15 min. The mixture was refluxed at 100°C for 24 h and then cooled to room temperature. After extraction with dichloromethane, the organic layer was washed with water and brine and dried over magnesium sulfate. The solvent was removed and the residue was purified by silica gel column chromatography (dichloromethane/hexane=1:5), followed by recrystallization from hexane to afford **3** (0.62 g, 64%) as white crystals. ^1H NMR (400 MHz, CDCl_3): δ =7.80–7.62 (m, 8H), 7.38–7.26 (m, 6H), 3.30–3.26 (t, J =6.8 Hz, 8H), 2.07–2.04 (q, 8H), 1.69–1.65 (m, 8H), 1.27–1.19 (q, 8H), 1.15–1.10 (q, 8H), 0.80–0.65 ppm (m, 8H); ^{13}C NMR (100 MHz, CDCl_3): δ =151.6, 151.0, 141.2, 141.0, 140.8, 127.5, 127.4, 126.6, 123.3, 121.7, 120.4, 120.2, 55.5, 40.6, 34.1, 33.0, 29.4, 28.1, 24.0 ppm; MS (MALDI-TOF): m/z (%): 982.11 [M].

2,7-Bis[9,9'-bis(6'-bromohexyl)fluorenyl]-4,4,5,5-tetramethyl[1.3.2]dioxaborolane (5): Compound **4** (2.38 g, 3.57 mmol), bis(pinacolato)diboron (2.72 g, 10.72 mmol), and potassium acetate (2.64 g, 26.8 mmol) were placed in a 100-mL round bottom flask. Anhydrous dioxane (60 mL) and $[\text{PdCl}_2(\text{dppf})]$ (0.18 g, 0.21 mmol) were added to the flask, and the reaction vessel was degassed for 15 min. The mixture was stirred at 80°C for 12 h under nitrogen. After the mixture had been cooled to room temperature, dioxane was removed by rotary evaporation. The residue was extracted with dichloromethane, and the organic phase was washed with water and brine, and dried over magnesium sulfate. The solvent was removed and the residue was purified by silica gel column chromatography (dichloromethane/hexane=1:2), followed by recrystallization from hexane to afford **5** (1.05 g, 52%) as white crystals. ^1H NMR (400 MHz, CDCl_3): δ =7.83–7.71 (m, 6H), 3.27–3.23 (t, J =6.9 Hz, 4H), 2.03–1.99 (m, 4H), 1.64–1.57 (q, J =7.0 Hz, 4H), 1.39(s, 24H), 1.17–1.13 (q, 4H), 1.06–1.02 (q, 4H), 0.71–0.67 ppm (q, 4H); ^{13}C NMR (100 MHz, CDCl_3): δ =150.3, 144.1, 134.0, 128.9, 119.7, 84.0, 55.2, 40.1, 34.2, 32.8, 29.2, 27.9, 23.6 ppm; MS (EI): m/z (%): 744 [M^+].

7-Bromo-9,9,9'-tetrakis(6'-bromohexyl)-2,2'-bifluorene (6): A flask containing compound **2** (2.54 g, 4.10 mmol), compound **4** (4.13 g, 6.19 mmol), and potassium carbonate (2.86 g, 20.75 mmol) in toluene (30 mL) and water (10 mL) was degassed for 15 min. $[\text{Pd}(\text{PPh}_3)_4]$ (0.011 g) was added to the flask and the mixture was degassed for another 15 min. The mixture was kept at approximately 100°C for 24 h and cooled to room temperature. After extraction with dichloromethane, the organic layer was washed with water and brine, and then dried over magnesium sulfate. The solvent was removed and the residue was purified by silica gel column chromatography (dichloromethane/hexane=1:5) followed by recrystallization from hexane to afford **6** (2.83 g, 65%) as a light-yellow solid. ^1H NMR (400 MHz, CDCl_3): δ =7.86–7.79 (m, 3H), 7.74–7.64 (m, 5H), 7.55 (s, 2H), 7.43–7.23 (m, 3H), 3.34–3.29 (t, J =6.4 Hz, 8H), 2.12–2.07 (m, 8H), 1.74–1.68 (m, 8H), 1.28–1.14 (m, 16H), 0.79–0.73 ppm (m, 8H); ^{13}C NMR (100 MHz, CDCl_3): δ =153.1, 151.4, 151.0, 150.8, 141.2, 140.9, 140.8, 140.4, 140.0, 139.5, 130.4, 129.3, 128.5, 127.5, 127.2, 126.7, 126.5, 126.4, 125.6, 123.1, 121.4, 120.4, 120.3, 120.1, 55.6, 55.3, 40.4, 34.2, 32.8, 29.2, 27.9, 23.8 ppm; MS (MALDI-TOF): m/z (%): 1061.61 [M].

9,9,9',9',9''-Hexakis(6'-bromohexyl)-2,2'-7',2''-terfluorene (7): Compound **7** was prepared according to the method for **6** by using compound **2** (2.54 g, 4.10 mmol), compound **4** (1.37 g, 2.05 mmol), potassium carbonate (2.86 g, 20.75 mmol), and $[\text{Pd}(\text{PPh}_3)_4]$ (30 mg) in toluene (20 mL) and water (10 mL). Column chromatography (hexane/dichloromethane=3:1) over silica gel yielded **7** (2.26 g, 75%) as an oily product. ^1H NMR (400 MHz, CDCl_3): δ =7.80–7.63 (m, 14H), 7.41–7.30 (m, 6H), 3.30–3.27 (t, J =6.4 Hz, 12H), 2.18–2.00 (m, 12H), 1.75–1.63 (q, 12H), 1.30–1.05 (m, 24H), 0.85–0.65 ppm (m, 12H); ^{13}C NMR (100 MHz, CDCl_3): δ =152.1, 151.8, 151.1, 141.1, 141.0, 140.5, 127.7, 126.5, 123.3, 121.8, 120.5, 120.4, 55.5, 40.6, 34.1, 33.0, 29.5, 28.2, 24.0 ppm; MS (MALDI-TOF): m/z (%): 1472.62 [M]; elemental analysis calcd (%) for $\text{C}_{75}\text{H}_{92}\text{Br}_6$: C 61.16, H 6.30; found: C 61.76, H 6.33.

7,7'-Dibromo-9,9,9'-tetrakis(6-bromohexyl)-2,2'-bifluorene (8): Compound **3** (1.13 g, 1.15 mmol) and dichloromethane (15 mL) were added

together in a 100-mL round bottom flask in an ice bath. Bromine (0.37 g, 2.30 mmol) in dichloromethane (10 mL) was added dropwise. The mixture was stirred at room temperature for 20 h. A diluted potassium hydroxide solution (3%, ca. 25 mL) was added to quench the reaction. The organic layer was separated and washed with water and brine and dried over magnesium sulfate. The solvent was removed and the residue was recrystallized in a mixture of dichloromethane and hexane to afford **8** (0.79 g, 60%) as a light-yellow solid. $^1\text{H NMR}$ (400 MHz, CDCl_3): δ = 7.80–7.49 (m, 12H), 3.30–3.27 (t, J = 6.8 Hz, 8H), 2.10–1.98 (m, 8H), 1.72–1.64 (q, J = 7.2 Hz, 8H), 1.30–1.06 (m, 16H), 0.75–0.65 ppm (m, 8H); $^{13}\text{C NMR}$ (100 MHz, CDCl_3): δ = 153.3, 151.3, 141.2, 140.2, 139.9, 130.6, 126.9, 126.6, 121.6, 120.6, 55.9, 40.5, 33.0, 29.4, 28.1, 24.0; MS (MALDI-TOF): m/z (%): 1139.89 [M].

7,7'-Dibromo-9,9,9',9',9''-hexakis(6-bromoheptyl)-2,2'-7',2'' terfluorene (9): Compound **9** was prepared according to the method for **8** by using compound **7** (1.08 g, 0.74 mmol) and bromine (0.37 g, 2.3 mmol). The product was purified using silica gel column chromatography (hexane/toluene = 3:1), which was followed by recrystallization from acetone at 4°C to afford **9** as a yellowish solid (0.54 g, 45%). $^1\text{H NMR}$ (300 MHz, CDCl_3): δ = 7.95–7.20 (m, 18H), 3.41–3.20 (m, 12H), 2.25–2.05 (m, 12H), 1.80–1.60 (m, 12H), 1.35–1.20 (m, 12H), 1.25–1.15 (m, 12H), 0.80–0.60 ppm (m, 12H); $^{13}\text{C NMR}$ (75 MHz, CDCl_3): δ = 152.9, 151.5, 150.8, 141.0, 140.4, 140.2, 139.8, 139.4, 130.2, 126.5, 126.4, 126.2, 121.3, 120.2, 55.5, 40.2, 33.9, 32.5, 29.1, 27.8, 25.0, 23.6 ppm; MS (MALDI-TOF): m/z (%): 1630.14 [M].

2-[9,9,9'-Tetrakis(6'-bromoheptyl)-7,2'-bifluorenyl-2-yl]-4,4,5,5-tetramethyl[1.3.2]dioxaborolan (10): Compound **10** was prepared according to the procedure used for **2** by using compound **6** (1.28 g, 1.20 mmol), bis(pinacolato)diboron (0.46 g, 1.81 mmol), potassium acetate (0.45 g, 4.52 mmol), and $[\text{PdCl}_2(\text{dppf})]$ (40 mg) in anhydrous dioxane (12 mL). Purification with silica gel column chromatography (hexane/toluene = 3:1) yielded **10** (0.78 g, 58%) as a white solid. $^1\text{H NMR}$ (400 MHz, CDCl_3): δ = 7.73–7.60 (m, 10H), 7.37–7.30 (m, 3H), 3.29–3.24 (t, J = 6.4 Hz, 8H), 2.09–2.04 (m, 8H), 1.70–1.61 (m, 8H), 1.40 (s, 12H), 1.25–1.05 (m, 16H), 0.75–0.60 ppm (m, 8H); $^{13}\text{C NMR}$ (100 MHz, CDCl_3): δ = 152.2, 151.5, 151.0, 150.2, 144.3, 141.5, 141.2, 141.0, 140.5, 134.5, 129.3, 128.1, 127.9, 127.4, 123.3, 121.7, 120.8, 120.4, 120.2, 119.5, 84.2, 55.6–55.5, 40.6–40.5, 34.1, 33.0, 29.5, 28.1, 25.4, 24.0–23.9 ppm; MS (MALDI-TOF): m/z (%): 1108.24 [M].

7,7'-Bis(4,4,5,5-tetramethyl[1.3.2]dioxaborolan-2-yl)-9,9,9'-tetra(6'-bromoheptyl)-2,2'-bifluorene (11): Compound **11** was prepared according to the procedure used for **5** by using compound **8** (2.6 g, 2.28 mmol), bis(pinacolato)diboron (1.73 g, 6.84 mmol), potassium acetate (1.69 g, 17.12 mmol), and $[\text{PdCl}_2(\text{dppf})]$ (0.12 g) in anhydrous dioxane (40 mL). Purification by using silica gel column chromatography (hexane/toluene = 3:1) yielded **11** (1.24 g, 44%) as a white solid. $^1\text{H NMR}$ (500 MHz, CDCl_3): δ = 7.81–7.61 (m, 12H), 3.28–3.25 (t, J = 7.0, 8H), 2.07–2.05 (m, 8H), 1.68–1.62 (q, J = 7.0, 8H), 1.41 (s, 24H), 1.22–1.19 (q, 8H), 1.10–1.08 (q, 8H), 0.72–0.67 ppm (q, J = 7.6, 8H); $^{13}\text{C NMR}$ (125 MHz, CDCl_3): δ = 151.8, 149.8, 143.8, 140.9, 140.3, 134.0, 128.8, 126.3, 121.3, 120.5, 119.2, 83.8, 55.2, 40.1, 33.9, 32.6, 29.0, 27.7, 25.0, 23.5 ppm; MS (MALDI-TOF): m/z (%): 1234.367 [M].

9,9,9',9',9'',9''',9''''-Octakis(6-bromoheptyl)-2,2'-7',2''-7''-tetrafluorene (12): Compound **12** was synthesized according to the same procedure for **7** by using compound **8** (468 mg, 0.41 mmol), compound **2** (506 mg, 0.82 mmol), potassium carbonate (675 mg, 4.93 mmol), and $[\text{PdCl}_2(\text{dppf})]$ (20 mg) in a mixture of toluene (8 mL) and water (3 mL). After reaction for 24 h at 85°C, the mixture was cooled down to room temperature. After evaporation of toluene, dichloromethane (ca. 20 mL) was added to the reaction mixture and the organic layer was washed with water followed by brine and then dried over magnesium sulfate. The solvent was removed and the residue was purified with silica gel column chromatography (dichloromethane/hexane = 1:4), followed by recrystallization from hexane to afford **12** (418 mg, 52%) as a pale yellow solid. $^1\text{H NMR}$ (400 MHz, CDCl_3): δ = 7.86–7.64 (m, 20H), 7.37–7.31 (m, 6H), 3.30–3.24 (t, J = 6.8 Hz, 16H), 2.18–2.05 (m, 16H), 1.72–1.64 (m, 16H), 1.31–1.10 (m, 32H), 0.90–0.65 ppm (m, 16H); $^{13}\text{C NMR}$ (100 MHz, CDCl_3): δ = 151.9, 151.6, 151.0, 141.2, 140.9, 140.5, 127.5, 127.4, 126.8, 126.6, 123.3,

121.7, 120.5, 120.2, 55.7–55.5, 40.6, 34.1, 33.0, 29.4, 28.1, 24.0 ppm; MS (MALDI-TOF) 1963.44 [M]; elemental analysis calcd (%) for $\text{C}_{100}\text{H}_{122}\text{Br}_8$: C 61.18, H 6.26; found: C 61.22, H 6.30.

9,9,9',9',9'',9''',9''''-Decakis(6'-bromoheptyl)-2,2'-7',2''-7''-2'''-7''',2''''-pentafluorene (13): Compound **13** was synthesized according to the same procedure used for **7** by using compound **6** (594 mg, 0.56 mmol), compound **5** (190 mg, 0.28 mmol), potassium carbonate (800 mg, 5.84 mmol), and $[\text{PdCl}_2(\text{dppf})]$ (15 mg) in a mixture of tetrahydrofuran (10 mL) and water (4 mL). After reaction for 24 h at 85°C, the mixture was cooled down to room temperature. After evaporation of tetrahydrofuran, dichloromethane (ca. 20 mL) was added to the reaction mixture, and the organic layer was washed with water followed by brine, and then dried over magnesium sulfate. The solvent was removed and the residue was purified with silica gel column chromatography (dichloromethane/hexane = 1:3) to afford **13** (200 mg, 27%) as a pale yellow solid. $^1\text{H NMR}$ (300 MHz, CDCl_3): δ = 7.95–7.60 (m, 26H), 7.45–7.30 (m, 6H), 3.31–3.27 (t, J = 6.6 Hz, 20H), 2.20–2.00 (m, 20H), 1.80–1.60 (m, 20H), 1.35–1.10 (m, 40H), 0.90–0.65 ppm (m, 20H); $^{13}\text{C NMR}$ (75 MHz, CDCl_3): δ = 151.4, 151.1, 150.6, 140.7, 140.4, 140.1, 127.1, 126.9, 122.8, 121.3, 121.2, 120.1, 120.0, 119.8, 55.3–55.1, 40.2, 34.0, 32.6, 29.0, 27.7, 23.7 ppm; MS (MALDI-TOF): m/z (%): 2453.93 [M]; elemental analysis calcd (%) for $\text{C}_{125}\text{H}_{152}\text{Br}_{10}$: C 61.19, H 6.24; found: C 61.08, H 6.26.

9,9,9',9',9'',9''',9''''-Dodecakis(6-bromoheptyl)-2,2'-7',2''-7''-2'''-7''',2''''-hexafluorene (14): Compound **14** was synthesized according to the same procedure for **7** by using compound **11** (239 mg, 0.19 mmol), compound **6** (411 mg, 0.39 mmol), potassium carbonate (820 mg, 6.00 mmol), tetrabutylammonium bromide (0.05 g), and $[\text{PdCl}_2(\text{dppf})]$ (15 mg) in a mixture of tetrahydrofuran (10 mL) and water (4 mL). After reaction for 24 h at 85°C, the mixture was cooled down to room temperature. After evaporation of tetrahydrofuran, dichloromethane (ca. 20 mL) was added to the reaction mixture, and the organic layer was washed with water followed by brine, and then dried over magnesium sulfate. The solvent was removed and the residue was purified with silica gel column chromatography (dichloromethane/hexane = 1:3) to afford **14** (170 mg, 30%) as a pale yellow solid. $^1\text{H NMR}$ (400 MHz, CDCl_3): δ = 7.89–7.63 (m, 32H), 7.36–7.31 (m, 6H), 3.31–3.27 (br, 24H), 2.20–2.00 (br, 24H), 1.70–1.60 (br, 24H), 1.27–1.10 (br, 48H), 0.90–0.65 ppm (br, 24H); $^{13}\text{C NMR}$ (100 MHz, CDCl_3): δ = 151.9, 151.6, 151.0, 141.2, 141.0, 140.5, 127.5, 127.4, 126.8, 126.6, 123.2, 121.8, 120.5, 120.2, 55.7–55.5, 40.6, 34.1, 33.0, 29.4, 28.1, 24.1–24.0 ppm; MS (MALDI-TOF): m/z (%): 2943.44 [M]; elemental analysis calcd (%) for $\text{C}_{150}\text{H}_{182}\text{Br}_{12}$: C 61.20, H 6.23; found: C 61.87, H 6.30.

9,9,9',9',9'',9''',9''''-Tetradecakis(6-bromoheptyl)-2,2'-7',2''-7''-2'''-7''',2''''-heptafluorene (15): Compound **15** was synthesized by using compound **9** (0.23 g, 0.14 mmol) and compound **10** (0.3 g, 0.28 mmol), according to the same procedure as for **14**, to yield **15** (0.13 g, 27%) as a yellowish solid. $^1\text{H NMR}$ (300 MHz, CDCl_3): δ = 7.85–7.35 (m, 44H), 3.30–3.20 (m, 28H), 2.20–2.05 (m, 28H), 1.70–1.67 (m, 28H), 1.28–1.18 (br, 56H), 0.85–0.70 ppm (m, 28H); $^{13}\text{C NMR}$ (75 MHz, CDCl_3): δ = 151.9, 151.5, 151.0, 141.0, 140.5, 127.0, 126.8, 123.2, 121.8, 120.5, 55.7, 40.6, 34.2, 33.0, 29.4, 28.1, 24.1 ppm; MS (MALDI-TOF): m/z (%): 3434.46 [M]; elemental analysis calcd (%) for $\text{C}_{175}\text{H}_{212}\text{Br}_{14}$: C 61.20, H 6.23; found: C 61.76, H 6.38.

9,9,9',9',9'',9''',9''''-Hexakis(6''-(N,N,N-trimethylammonium)heptyl)-2,2'-7',2''-terfluorenyl hexabromide (16): Condensed trimethylamine (ca. 2 mL) was added dropwise to a solution of compound **7** (1.0 g, 0.68 mmol) in THF (15 mL) at –78°C. The mixture was allowed to warm up to room temperature. The precipitate was re-dissolved by the addition of methanol (10 mL). After the mixture was cooled down to –78°C, extra trimethylamine (ca. 2 mL) was added and the mixture was stirred for 24 h at room temperature. After the solvent had been removed, acetone was added to precipitate **16** (0.75 g, 60%) as a light yellow powder. $^1\text{H NMR}$ (300 MHz, CD_3OD): δ = 8.46–8.32 (m, 14H), 8.00–7.88 (m, 6H), 3.83–3.77 (br, 12H), 3.58 (s, 54H), 2.85–2.60 (br, 12H), 2.12 (br, 12H), 1.70 (br, 12H), 1.35–1.10 ppm (br, 12H); $^{13}\text{C NMR}$ (75 MHz, CD_3OD): δ = 152.9, 152.5, 151.9, 142.2, 142.0, 141.6, 128.4, 128.2, 127.4, 124.1, 122.2, 121.4, 120.9, 67.6, 56.7, 53.6, 41.3, 30.3, 26.9, 25.0, 23.8 ppm; MS

- [21] a) B. S. Harrison, M. B. Ramey, J. R. Reynolds, K. S. Schanze, *J. Am. Chem. Soc.* **2000**, *122*, 8561–8562; b) C. Tan, M. R. Pinto, K. S. Schanze, *Chem. Commun.* **2002**, 446–447; c) M. R. Pinto, B. M. Kristal, K. S. Schanze, *Langmuir* **2003**, *19*, 6523–6533.
- [22] a) D. T. Mcquade, A. E. Pullen, T. M. Swager, *Chem. Rev.* **2000**, *100*, 2537–2574; b) S. W. Thomas III, G. D. Joly, T. M. Swager, *Chem. Rev.* **2007**, *107*, 1339–1386.
- [23] J. R. Lakowicz, *Principle of Fluorescence Spectroscopy*, **1999**, Plenum, New York.
- [24] Q. H. Xu, B. S. Gaylord, S. Wang, G. C. Bazan, D. Moses, A. J. Heeger, *Proc. Natl. Acad. Sci. USA* **2004**, *101*, 11634–11639.

Received: December 4, 2007

Revised: April 29, 2008

Published online: July 11, 2008